Vuyyuru, Sravan Kumar Reddy; Valkonen, Risto; Kwon, Do-Hoon; Tretyakov, Sergei

Efficient Anomalous Reflector Design Using Array Antenna Scattering Synthesis

Published in:
IEEE Antennas and Wireless Propagation Letters

DOI:
10.1109/LAWP.2023.3260920

Published: 01/07/2023

Document Version
Peer reviewed version

Please cite the original version:
Vuyyuru, S. K. R., Valkonen, R., Kwon, D-H., & Tretyakov, S. (2023). Efficient Anomalous Reflector Design Using Array Antenna Scattering Synthesis. *IEEE Antennas and Wireless Propagation Letters* , *22*(7), 1711-1715. https://doi.org/10.1109/LAWP.2023.3260920

Efficient Anomalous Reflector Design Using Array Antenna Scattering Synthesis

Sravan K. R. Vuyyuru, *Member, IEEE,* Risto Valkonen, *Member, IEEE,*
Do-Hoon Kwon, *Senior Member, IEEE,* and Sergei A. Tretyakov, *Fellow, IEEE*

***Abstract*—A perfect anomalous reflector is designed by employing the receiving and scattering array antenna theory to optimize the scattering characteristics of a planar reflecting surface. For periodic reflectors with a supercell consisting of a relatively few reactively loaded radiating elements, reflection amplitudes into propagating Floquet modes are controlled in an algebraic optimization of the load reactances, avoiding brute-force optimization via electromagnetic simulations. Wide-angle reflectors are numerically designed and compared with the conventional reflectarray designs, showing that the proposed design approach achieves reflection efficiencies higher than the linear reflection phase gradient method in a computationally efficient manner.**

***Index Terms*—Reconfigurable Intelligent Surface (RIS), anomalous reflector, phased arrays, receiving antennas**

I. Introduction

A RECONFIGURABLE Intelligent Surface (RIS) is an artificial two-dimensional planar surface designed to control electromagnetic (EM) scattering characteristics both dynamically and intelligently. In particular, RIS as an anomalous reflector comprises a flat surface with an abundance of discrete elements having controllable properties, which can manipulate the EM properties of the reflected signal, such as the amplitude, phase, and polarization, to enhance multiple functionalities [1]. However, the research is still in the early stage of developing an efficient RIS with anomalous reflection.

Implementing anomalous phase-gradient reflectors unveils the inherent complication of a trade-off between a large deflection angle and the power efficiency [2]. When the traditional reflectarray antenna design approach [3] or, equivalently, the generalized law of reflection [4] is employed, the power efficiency of plane-wave reflection into a predetermined nonspecular direction diminishes gradually for large deflection tilts [5]. On top of the suboptimal theoretical efficiencies, losses associated with practical tuning elements in RISes further decrease the efficiency [6].

Spatially dispersive metasurfaces that exhibit nonlocal reflection properties can achieve nominally perfect wide-angle reflection. Arrays of printed patches were optimized using full-wave EM simulations, and a high reflection efficiency was experimentally validated [5]. For a periodic reflector configuration that allows two propagating Floquet modes, perfect anomalous reflection using two meta-atoms in a supercell period was designed using simulation and experimentally confirmed [7]. Designing a large-scale finite reflector based on the conventional reflectarray design method compromises the reflection efficiency for large deflection angles. On the other hand, while perfect wide-angle reflection can be anticipated, a design process for individualized meta-atoms using full-wave EM simulations is not efficient, demanding large computational resources and long optimization times.

In this letter, we introduce an algebraic optimization method that can be used for periodic perfect anomalous reflectors comprising a few reactively loaded printed microstrip patches in a supercell. Example arrays are designed for high nonspecular reflection efficiency via efficient synthesis of the scattered Floquet modes. Computationally-intensive full-wave EM simulations are avoided by formulating the reflected wave synthesis as an algebraic optimization for the load reactance values. Reflector design based on surface field optimization leads to an algebraic optimization problem [8], but its realization requires meta-atoms in a deep subwavelength scale. Numerical reflector designs for 41.81°, 70°, and 80° deflection angles in TE polarization using three- and four-patch supercell arrays demonstrate the efficient design process and high reflection efficiencies.

II. Reception and Scattering by Loaded Phased Arrays

The scattering characteristics of a load-terminated antenna depend on the load connected to the antenna terminals [9], [10]. The total scattered E-field, $\mathbf{E}^s$, scattered by an antenna with a load impedance Z_L is given by the sum of zero-current scattering and port-current scattering contributions as [11]

$$\mathbf{E}^s(Z_L) = \mathbf{E}^s(Z_L = \infty) - I_L \mathbf{E}_I, \tag{1}$$

where $\mathbf{E}_I$ is the E-field in the transmitting (TX) mode for unit input current excitation, and I_L is the load current. Other decompositions of the total scattered field are also possible [11], [12].

This work was supported in part by the European Union's Horizon 2020 MSCA-ITN-METAWIRELESS project, under the Marie Skłodowska-Curie grant agreement No 956256 and in part by the US Army Research Office under grant W911NF-19-2-0244.

S. K. R. Vuyyuru is with Nokia Bell Labs, Karakaari 7, 02610 Espoo, Finland and the Department of Electronics and Nanoengineering, School of Electrical Engineering, Aalto University, 02150 Espoo, Finland (e-mail: sravan.vuyyuru@nokia.com; sravan.vuyyuru@aalto.fi).

R. Valkonen is with Nokia Bell Labs, Karakaari 7, 02610 Espoo, Finland (e-mail: risto.valkonen@nokia-bell-labs.com).

D.-H. Kwon is with the Department of Electrical and Computer Engineering, University of Massachusetts Amherst, Amherst, MA 01003, USA (e-mail: dhkwon@umass.edu).

S. A. Tretyakov is with the Department of Electronics and Nanoengineering, School of Electrical Engineering, Aalto University, 02150 Espoo, Finland (e-mail: sergei.tretyakov@aalto.fi).

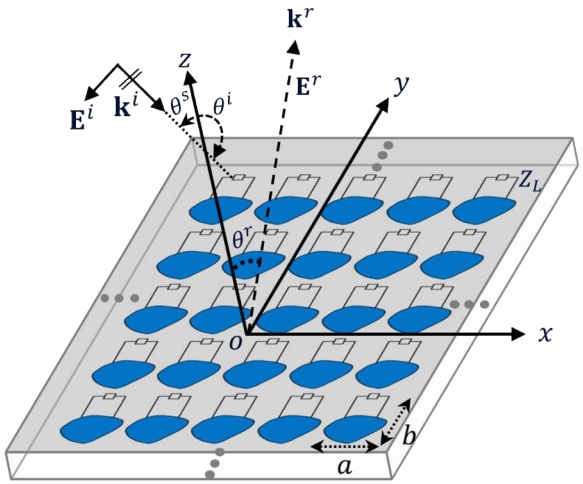

Fig. 1: An infinite planar array under a plane wave illumination, with unit cell spacing a and b in the x- and y-axis directions, respectively.

The linearity relation (1) also applies to receiving (RX) antenna arrays. Consider an infinite periodic RX array of identical loaded elements on a rectangular grid backed by a perfect electric conductor (PEC) ground plane, as illustrated in the Fig. 1. A complex Z_L terminates each unit element. The array spans around the coordinate system origin O in the xy-plane with a and b as the unit cell dimensions along the x- and y-directions, respectively. In an $e^{j\omega t}$ time convention, the array is subject to an incident plane wave with an E-field $\mathbf{E}^i = \mathbf{E}_0^i e^{-j\mathbf{k}^i\cdot\mathbf{r}}$, where $\mathbf{r} = \hat{x}x + \hat{y}y + \hat{z}z$ and the incident k-vector, $\mathbf{k}^i$, is defined by the direction (θ^i, ϕ^i). Via reciprocity, this is associated with the array in the TX mode scanning in the direction $(\theta^s, \phi^s) = (\pi - \theta^i, \phi^i - \pi)$.

For each RX array element, the open-circuit voltage and the load current expressions take the same form as for an isolated RX antenna [13]:

$$V_{\text{oc}}^{\text{el}} = \mathbf{h}^{\text{el}}(\theta^s, \phi^s) \cdot \mathbf{E}^i(O), \tag{2}$$

$$I_L = \frac{V_{\text{oc}}^{\text{el}}}{Z_A + Z_L}, \tag{3}$$

where $\mathbf{h}^{\text{el}}$ is the element vector effective height and Z_A is the element input impedance under the scan condition in (θ^s, ϕ^s). From a TX-mode simulation, $\mathbf{h}^{\text{el}}$ can be found as a function of direction from the vector element pattern with complex-valued components.

For any propagating Floquet mode, the complex scattered plane-wave amplitude associated with a given Z_L can be found using (1). Consider a reflected plane wave with an E-field, $\mathbf{E}^s = \mathbf{E}_0^s e^{-j\mathbf{k}^r\cdot\mathbf{r}}$, where the k-vector $\mathbf{k}^r$ points in the direction (θ^r, ϕ^r). When no grating lobes are present, only the specular reflection direction is possible for $\mathbf{k}^r$. For the loaded array, we have [13]

$$\mathbf{E}_0^s(Z_L) = \mathbf{E}_0^s(Z_L = \infty) - \frac{k\eta I_L}{2abk_{z0}}\mathbf{h}^{\text{el}}(\theta^r, \phi^r), \tag{4}$$

where k is the free-space wavenumber, $\eta \approx 377\ \Omega$ is the free-space intrinsic impedance, and $k_{z0} = k\cos\theta^r$.

Using (2)–(4), finding the scattered plane-wave amplitude for an arbitrary load Z_L requires solving a linear equation. Separate full-wave simulation is avoided. The reflection properties are characterized in four reflection coefficients

$$\Gamma_{\alpha\beta} = \frac{\hat{e}_\alpha^r \cdot \mathbf{E}_0^s}{\hat{e}_\beta^i \cdot \mathbf{E}_0^i};\ \alpha, \beta = \text{TM or TE}, \tag{5}$$

where

$$\hat{e}_{\text{TM}}^{\{i,r\}} = \frac{\mathbf{k}_t^{\{i,r\}}}{|\mathbf{k}_t^{\{i,r\}}|},\ \hat{e}_{\text{TE}}^{\{i,r\}} = \frac{\hat{z}\times\mathbf{k}_t^{\{i,r\}}}{|\mathbf{k}_t^{\{i,r\}}|} \tag{6}$$

with $\mathbf{k}_t^{\{i,r\}} = \mathbf{k}^{\{i,r\}} - \hat{z}(\hat{z}\cdot\mathbf{k}^{\{i,r\}})$.

III. Scattering Synthesis for Periodically Loaded Arrays

To design a periodic anomalous reflector, the unit cell in Section II can be extended to a supercell containing a few loaded elements. Consider a supercell consisting of N loaded meta-atoms, supporting propagating Floquet modes indexed by m, and treat it as a linear N-port network. We extend (3) into matrix form to find the N induced port currents as

$$\mathbf{I}_L = (\mathbf{Z}_A + \mathbf{Z}_L)^{-1}\mathbf{V}_{\text{oc}}, \tag{7}$$

where $\mathbf{Z}_A$ is the $N \times N$ impedance matrix of the supercell array, and $\mathbf{Z}_L$ is a diagonal matrix with N individual load impedance values. The $N \times 1$ column vector $\mathbf{V}_{\text{oc}}$ has the open-circuit RX voltages at individual element terminals. The $N\times 1$ column vector $\mathbf{I}_L$ contains all individual port currents. In preparation for numerical optimization for a desired scattering response by optimizing the load impedance values, preliminary simulation studies are needed. A set of TX simulations are needed to find the array impedance matrix $\mathbf{Z}_A$ and the element vector effective height for the n-th element, $\mathbf{h}_n^{\text{el}}$. The N open-circuit RX voltages can be found using (2) for each of the N elements. Alternatively, an RX-mode simulation can be performed to find all open-circuit voltages.

For a given set of load impedances represented by $\mathbf{Z}_L$, the amplitude $\mathbf{E}_m^s$ of the reflected plane wave of the m-th propagating Floquet mode propagating in (θ_m^r, ϕ_m^r) is found by extending (4) as

$$\mathbf{E}_m^s(\mathbf{Z}_L) = \mathbf{E}_m^s(\mathbf{Z}_L = \infty) - \sum_{n=1}^{N}\frac{k\eta I_{Ln}}{2abk_{zm}}\mathbf{h}_n^{\text{el}}(\theta_m^r, \phi_m^r), \tag{8}$$

where I_{Ln} is the load current at the n-th port and $k_{zm} = k\cos\theta_m^r$. For the m-th reflected harmonic, the reflection coefficients are defined by (5) using $(\theta^r, \phi^r) = (\theta_m^r, \phi_m^r)$.

We aim to realize anomalous reflection only in the plane of incidence (the xz-plane). For periodically loaded arrays, the x-component of the m-th Floquet harmonic is

$$k_{xm} = k_{x0} + \frac{2m\pi}{D_x}, \tag{9}$$

where $k_{x0} = k\sin\theta^i$. The supercell dimension $D_x = a$ along the x-axis is chosen such that the anomalous direction corresponds to a $m = +1$ or $m = -1$ harmonic [14]. It is preferable to select a smallest value to avoid the unwanted propagating channels.

For perfect anomalous reflection, we choose to maximize the power efficiency into the desired anomalous direction using

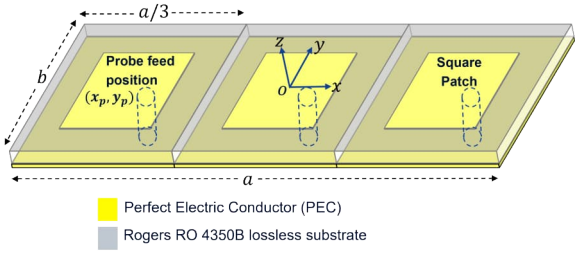

Fig. 2: A three-patch supercell geometry of an infinite periodic anomalous reflector.

TABLE I: Dimensions of the supercell array

Parameters	$\theta^r(^\circ)$	3-Patch supercell	4-Patch supercell
Supercell dimension $(a \times b)$	41.81	$1.5\lambda \times 0.5\lambda$	$1.5\lambda \times 0.375\lambda$
	70	$1.064\lambda \times 0.3547\lambda$	$1.064\lambda \times 0.266\lambda$
	80	$1.0154\lambda \times 0.3385\lambda$	$1.0154\lambda \times 0.2539\lambda$
Patch dimension	41.81	$0.2468\lambda \times 0.2468\lambda$	$0.248\lambda \times 0.248\lambda$
	70	$0.2471\lambda \times 0.2471\lambda$	$0.2267\lambda \times 0.2267\lambda$
	80	$0.2458\lambda \times 0.2458\lambda$	$0.2211\lambda \times 0.2211\lambda$
Probe position (x_p, y_p)	41.81	$(0, 0.671)$ mm	$(0, 1.0134)$ mm
	70	$(0, 1.1093)$ mm	$(0, 1.1589)$ mm
	80	$(0, 1.23)$ mm	$(0, 1.0978)$ mm

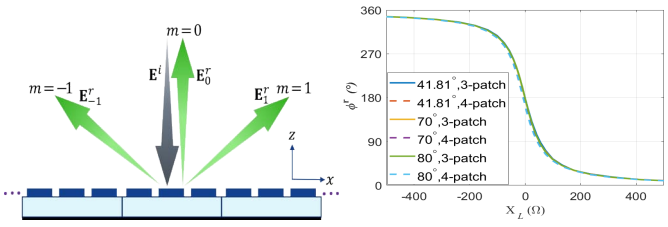

(a) (b)

Fig. 3: Anomalous reflection for normal incidence in 2-D TE polarization. (a) Schematic representation of three propagating harmonics for 3-patch supercell. (b) Design curve for the reflection phase ϕ^r in the traditional reflectarray design

TABLE II: Summary of the optimized designs and comparison with the traditional reflectarray approach.

Supercell	$\theta^r(^\circ)$	Optimized load reactances (Ω)	Opt (%)	refl (%)
3-patch	41.81	$-103,\ 63,\ -1$	99	94.4
	70	$34,\ -40,\ 138$	85.3	67.5
	80	$45,\ -40,\ 125$	75.3	42.2
4-patch	41.81	$-40,\ -10,\ 50,\ 320$	99.5	96.4
	70	$31,\ 11,\ 322,\ -226$	99.8	63
	80	$79,\ 30,\ 616,\ -244$	99.7	37.3

hierarchical clustered-based optimization, while leaving the reflection phase as a free parameter. The design parameters are the reactive loads. Although nonlinear, this optimization is of algebraic nature, which is significantly more efficient than EM simulation-based optimizations.

IV. Numerical Example

Anomalous reflectors for TE polarization under normal incidence ($\theta^i = 0^\circ$) are designed. We select the supercell periodicity to be $D_x = \lambda/\sin\theta^r$ allowing only one propagating harmonic on each side of the surface normal in the x-direction. We choose, as a baseline, a 3-patch supercell with a half-wave element spacing, which leads to $\theta^r = 41.81^\circ$ and $D_x = 1.5\lambda$. To demonstrate higher deflection angles, we also consider $\theta^r = 70^\circ$ and 80°, associated with $D_x = 1.064\lambda$ and 1.0154λ, respectively. Given by $|k_{xm}| < k$, only three modes with $m = 0, \pm 1$ correspond to propagating harmonics, as illustrated in Fig. 3(a). All higher-order modes are evanescent. The fitness to maximize toward unity in optimization is the power reflection efficiency ζ for $m = +1$, given by

$$\zeta = \frac{\cos\theta_1^r}{\cos\theta^i}\left|\frac{\hat{e}^r_{\text{TE}}\cdot\mathbf{E}^s_1}{\hat{e}^i_{\text{TE}}\cdot\mathbf{E}^i_0}\right|^2 \quad (\theta_1^r = \theta^r). \tag{10}$$

We start with determining the dimensions for a single patch unit cell that occupies a size of $a/3\times b$ using periodic boundary conditions to obtain a resonant patch element. All numerical simulations have been obtained using CST Microwave Studio. At a design frequency of 28 GHz, a linearly polarized square PEC patch antenna is designed as a doubly-periodic array for a broadside scan with a good impedance match to 50 Ω. The substrate is given by a Rogers RO4350B laminate (a relative permittivity $\epsilon_r = 3.66$) without loss and a 0.338-mm thickness. Next, a supercell by cascading patches along the x-axis direction is formed, as illustrated in Fig. 2 for a three-patch case. The patch dimensions, feeding points, and supercell details optimized for resonance at the design frequency are listed in Table I for the three proposed deflection angles. Now, individual reactive loads connected to the patch ports are optimized following Section III. The optimized load reactance values and the associated values of ζ are listed in Table II.

For reference and comparison, periodic loaded three-patch and four-patch supercell arrays are also designed following the traditional phase-gradient reflectarray design approach using the locally periodic approximation [3]. For that purpose, a design curve between the reflection phase and the load reactance is obtained by simulating a single loaded patch under periodic boundary conditions at normal incidence, as plotted in Fig. 3(b). Then, the reference reflector is defined by a set of three or four reactive loads in a supercell determined to provide an x-linear reflection phase gradient associated with the anomalous deflection angle, read off of the design curve.

Figure 4(a) plots ζ of the optimized designs, compared against the phase-gradient design. We allow the anomalous reflection phase, $\phi^r = \angle\Gamma_{\text{TE-TE}}$, to be any value in maximizing ζ for both the proposed and traditional phase-gradient methods. The efficiency numbers for both the proposed technique and the reflectarray method are similarly high in the $\theta^r = 41.81^\circ$ case with three- as well as four-patch supercells. Since the deflection angle for the 1.5λ period is moderate, the locally-periodic phase-gradient design outcomes are acceptable. However, the power efficiencies of the reflectarray approach with $D_x = 1.064\lambda$ and 1.0154λ drop with larger θ^r, and stay below the numerically estimated limit (solid blue) associated with a reactive surface with an x-continuous linear reflection

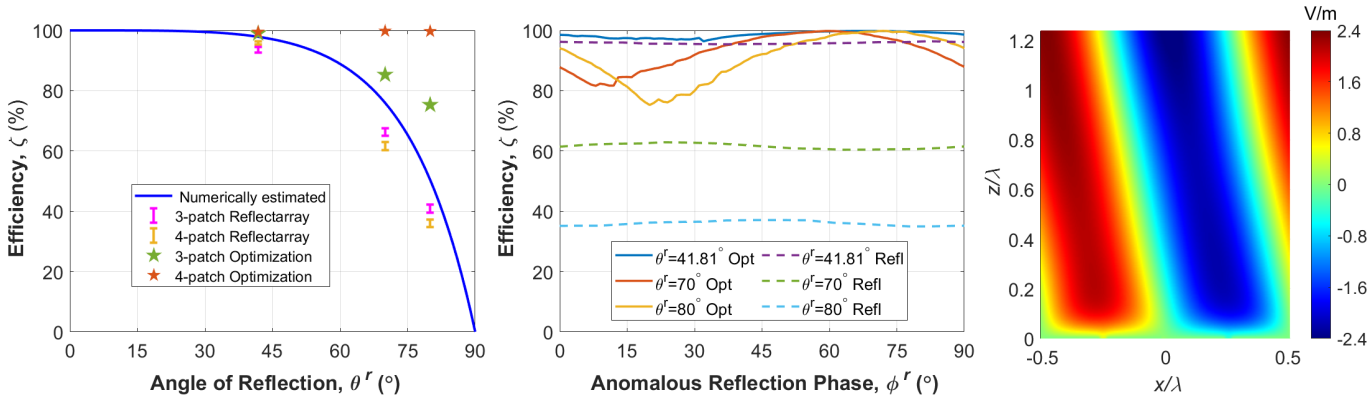

Fig. 4: Simulated performance of the anomalous reflector designs. (a) Power efficiency comparison for the optimized and conventional reflectarray designs for $\theta^r = 41.81°$, 70°, and 80° with three- and four-patch supercells. The blue line represents the efficiency limit for a conventional lossless reflector. Over all possible reflection phase angles, bars indicate the range of efficiencies. (b) Reflection efficiency with respect to ϕ^r for the four-patch supercell case. The efficiencies repeat themselves every 90° of the reflection phase. (c) Snapshot at time $t = 0$ of the y-component of the scattered E-field, $\mathrm{Re}\{E_y^s(x, z)\}$, in the plane of incidence for the 80° deflector with a four-patch supercell under a unit-plane wave illumination at normal incidence.

phase [2], [15]. For the three-element supercell configurations, the proposed method achieves higher efficiencies than the linear phase gradient limit, but fails to closely approach the ideal 100% (green stars). When the supercell contains four load-adjusted patches, the proposed method finds optimal sets of reactive loads that achieve nominally perfect efficiencies in excess of 99% (red stars).

The maximum efficiency behavior with respect to the number of patches may be understood qualitatively using the required number of sources in controlling Floquet modes. According to [16], the number of passively induced sources to exactly control three Floquet modes arbitrarily in this design are six. However, the 3×3 scattering matrix of a lossless system is unitary. Hence, it will take less than six passive loads to achieve perfect deflection. Further, it can be conjectured that relaxing one condition in controlling Floquet modes may further reduce the required number of loaded elements. Within the unitary property of the S-matrix, we can allow the reflection phase to have any value. For ϕ^r swept from 0° to 90°, reflectors are designed using the conventional and proposed techniques for $\theta^r = 41.81°$, 70°, and 80°. The simulated reflection efficiencies are plotted in Fig. 4(b) for four-patch supercell configuration. The efficiencies for the traditional reflectarray vary weakly with respect to ϕ^r. For the proposed approach, ζ reaches 100% only at specific values of ϕ^r. The proposed technique consistently achieves a higher efficiency than the reflectarray approach at all ϕ^r. This is attributed to two features of the proposed technique: the efficiency metric is directly maximized by optimization, and mutual coupling is accurately taken into account. In contrast, not only is the linear reflection phase gradient suboptimal for large deflection angles [2], but the mutual coupling model in the reflectarray approach becomes inaccurate for inhomogeneously-loaded arrays.

Star markers in Fig. 4(a) are CST-simulated efficiencies of the designs associated with maximum efficiencies in Fig. 4(b). The predicted results using array scattering synthesis agree well with CST simulations. Table II summarizes the simulated efficiencies for the reflectarray and optimized designs shown in Fig. 4(a). For the optimized 80° reflector with a four-patch supercell under a unit plane-wave ($\mathbf{E}_0^i = \hat{y}$ V/m) illumination, Fig. 4(c) plots a snapshot of the scattered E-field component, E_y^s. Away from the $z = 0$ reflector plane, a pure plane wave propagating in the $\theta^r = +80°$ direction is observed, as desired.

It is worth mentioning that in the infinite periodic array, the precise angle of anomalous reflection direction depends on the frequency, $\sin\theta^r = \lambda/D_x$. However, admitting a small beam pointing error, a decent 1-dB efficiency bandwidth of anomalous reflection can be achieved for, e.g., a 5G NR channel bandwidth up to 800 MHz according to frequency-swept simulations with 4-patch supercell designs.

In any chosen load optimization technique, the proposed method evaluates ζ using an algebraic process for each candidate design. For periodic reflectors comprising a few loaded elements in a supercell, this evaluation is nearly instant, significantly enhancing the overall numerical efficiency of optimization over simulation-based techniques.

V. Conclusion

A numerically efficient design technique for planar anomalous reflectors based on array antenna scattering synthesis has been presented. For periodic reflectors comprising impedance-loaded elements, the reflected plane wave amplitude in each propagating channel is expressed as a superposition of zero-port-current scattering and individual port-current contributions. Maximizing the anomalous reflection efficiency is cast as an algebraic optimization problem, solving which is numerically efficient compared with traditional EM simulation-based approaches. While the design technique has been developed and validated for infinite periodic arrays in TE polarization, the approach may be extended to finite arrays, TM polarization, or anomalous reflection directions off the incidence plane.

REFERENCES

[1] M. Di Renzo, A. Zappone, M. Debbah, M.-S. Alouini, C. Yuen, J. de Rosny, and S. Tretyakov, "Smart radio environments empowered by reconfigurable intelligent surfaces: How it works, state of research, and the road ahead," *IEEE J. Sel. Areas Commun.*, vol. 38, no. 11, pp. 2450–2525, 2020.

[2] V. S. Asadchy, M. Albooyeh, S. N. Tcvetkova, A. Díaz-Rubio, Y. Ra'di, and S. Tretyakov, "Perfect control of reflection and refraction using spatially dispersive metasurfaces," *Phys. Rev. B*, vol. 94, no. 7, p. 075142, 2016.

[3] J. Huang and J. A. Encinar, *Reflectarray Antennas*. Hoboken, NJ, USA: Wiley, 2008.

[4] N. Yu, P. Genevet, M. A. Kats, F. Aieta, J.-P. Tetienne, F. Capasso, and Z. Gaburro, "Light propagation with phase discontinuities: generalized laws of reflection and refraction," *Science*, vol. 334, pp. 333–337, Oct. 2011.

[5] A. Díaz-Rubio, V. S. Asadchy, A. Elsakka, and S. A. Tretyakov, "From the generalized reflection law to the realization of perfect anomalous reflectors," *Sci. Adv.*, vol. 3, no. 8, p. e1602714, 2017.

[6] A. Casolaro, A. Toscano, A. Alu, and F. Bilotti, "Dynamic beam steering with reconfigurable metagratings," *IEEE Trans. Antennas Propag.*, vol. 68, no. 3, pp. 1542–1552, 2019.

[7] A. M. H. Wong and G. V. Eleftheriades, "Perfect anomalous reflection with a bipartite Huygens' metasurface," *Phys. Rev. X*, vol. 8, 2018, Art. No. 011036.

[8] D.-H. Kwon, "Lossless scalar metasurfaces for anomalous reflection based on efficient surface field optimization," *IEEE Antennas Wireless Propag. Lett.*, vol. 17, no. 7, pp. 1149–1152, Jul. 2018.

[9] C. A. Balanis, *Antenna Theory: Analysis and Design*. John wiley & sons, 2015.

[10] W. L. Stutzman and G. A. Thiele, *Antenna Theory and Design*. John Wiley & Sons, 2012.

[11] R. Collin, "Limitations of the Thevenin and Norton equivalent circuits for a receiving antenna," *IEEE Antennas Propag. Mag.*, vol. 45, no. 2, pp. 119–124, 2003.

[12] R. C. Hansen, "Relationships between antennas as scatterers and as radiators," *Proc. IEEE*, vol. 77, no. 5, pp. 659–662, May 1989.

[13] D.-H. Kwon, "Effective height, receiving area, and receiving efficiency of infinite planar phased array elements," *IEEE Trans. Antennas Propag.*, vol. 63, no. 5, pp. 2022–2031, 2015.

[14] V. S. Asadchy, A. Díaz-Rubio, S. N. Tcvetkova, D.-H. Kwon, A. Elsakka, M. Albooyeh, and S. A. Tretyakov, "Flat engineered multichannel reflectors," *Phys. Rev. X*, vol. 7, 2017, Art. No. 031046.

[15] V. S. Asadchy, A. Wickberg, A. Díaz-Rubio, and M. Wegener, "Eliminating scattering loss in anomalously reflecting optical metasurfaces," *ACS Photon.*, vol. 4, no. 5, pp. 1264–1270, 2017.

[16] V. Popov, F. Boust, and S. N. Burokur, "Constructing the near field and far field with reactive metagratings: Study on the degrees of freedom," *Phys. Rev. Appl.*, vol. 11, Feb 2019, Art. No. 024074.